Environ Earth Sci (2016) 75:1310
DOI 10.1007/s12665-016-6113-4

ORIGINAL ARTICLE

Rock fall hazard assessment in Asar Hill, ancient Mabolla City, Mugla—SW Turkey

Murat Gül[1] · Ahmet Özbek[2] · Ergun Karacan[1]

Received: 27 August 2015 / Accepted: 23 September 2016 / Published online: 1 October 2016
© Springer-Verlag Berlin Heidelberg 2016

Abstract This paper discusses the potential rock fall hazard of Asar Hill. This flat-topped hill, containing Upper Miocene conglomerate and finer-grained sedimentary rocks, hosts to the ancient Mabolla City. The seasonal temperature differences are high in this rainy region. Block sizes, bed, and joints attitudes were measured along three profiles during field study. Schmidt Hammer was applied to grains and matrix of conglomerates for determining strength in situ. One joint set in Profile A, 3 in Profile B, and 4 in Profile C were determined via dips analysis. An intersection of joints and bedding (directed 25°–35°NW) caused the block formation, control slope, angle and mass movement type. At least 10 blocks (0.6–1241.085 tons) were fixed on top of profiles. Two blocks on top of the eastern Profile A contain archaeological ruins. After back analysis for determining restitution coefficients, RocFall version 4.9 software program was used to determine possible end points of those blocks. Most of the blocks can reach the valley and pass the other side, which includes settlements and gardens. Consequently the possible rock fall hazard in Asar hill is threatening visitors and settlers. The cleaning of detached blocks on top of slope is one of the easiest ways. However, in situ preservation of blocks with archaeological ruins via tensioned rock anchors and/or patterned rock bolts has vital importance. Relocation of settlers and gardens, opening trench around hill, and establishing green belt-forest would be considered as other measures.

Keywords Conglomerate · Schmidt hammer · Kinematic analyses · Rock fall · Mugla—Turkey

✉ Murat Gül
muratgul@mu.edu.tr

[1] Department of Geological Engineering, Engineering Faculty, Mugla Sıtkı Koçman University, 48100 Kötekli-Muğla, Turkey

[2] Department of Geological Engineering, Kahramanmaraş Sutcu Imam University, Avsar Campus, Kahramanmaraş, Turkey

Introduction

Mass wasting can damage property and people's life (Hermanns et al. 2006; Tang et al. 2014). Hence understanding, evaluating, monitoring, and mitigating these movements have vital importance for protection of recent civilization and understanding formation of recent geomorphology (Ocakoglu et al. 2009; Alemdağ et al. 2014; Tang et al. 2014). Mass movements are classified based on the type of material and velocity of movement (Varnes 1978; Hungr et al. 2014).

Rock fall is one of the examples of rapid mass movement, which occurs in front of steep slope, rocky hill and formed via free leaping, bounding or rolling of one or a few boulders–blocks (Varnes 1978; Yılmaz et al. 2008; Keskin 2013; Li and Lan 2015). The rock fall formed depends on an intersection of joints, wave notch erosion, physical–chemical–biological weathering, freeze–thaw cycles weathering, shaking of ground via seismic activities, and excavation of road, quarry, or foundation (Wasowski and Gaudio 2000; Agliardi and Crosta 2003; Frayssines and Hantz 2006, 2009; Koleini and Van Rooy 2011; Topal et al. 2012; Wei et al. 2014). The dynamic properties of rock fall may be affected by geometrical features, slope height, slope angles, mechanical properties (friction, roughness, etc.), lithological properties of slope, and block properties such as size, shape, and weight (Agliardi and

Crosta 2003; Topal et al. 2012; Fityus et al. 2013). Rock fall can be observed in different lithology and different environments (Fityus et al. 2013). Sometimes, they affect ancient ruins generally at the top of hill (Topal et al. 2012; Korkanç et al. 2014).

The assessment of rock fall can make via different ways and using different information. Some studies used geomorphological features, aerial photographs, seismic reflection profile, and finite element analysis (Frayssines and Hantz 2006; Hermanns et al. 2006; Keskin 2013). Structural properties determination, kinematic analysis, and zoning map preparation were also used for rock fall assessment (Koleini and Van Rooy 2011; Saroglou et al. 2012; Keskin 2013). RocFall software is successfully applied for assessment of the potential rock fall hazard in different part of world for different environment, for example, historical places in Afyon—Turkey (Topal et al. 2006); dam construction in Marun Dam, Iran (Koleini and Van Rooy 2011); Monemvasia historical site located in Peloponnese in Southern Greece (Saroglou et al. 2012); Kastamonu Castle in Turkey (Topal et al. 2012); urban areas in Erzincan—Turkey (Keskin 2013); road construction–excavation in Taiwan (Wei et al. 2014); touristic coastal area in Kuşadası, Aydın, Turkey (Kaya and Topal 2015); and road construction–excavation in Saudi Arabia (Sadagah 2015).

The Asar Hill is located in north of Mugla city centre (Fig. 1). The information board at the top of the Asar Hill reported that Asar Hill host ancient city wall (dated before the fourth century BC), Hellenistic city wall, open-air sanctuary, rock-cut house, rock-cut tomb (belong to Roman Period), Byzantine city walls, niches for cremation burials and cistern. According to archaeological excavation by the Tourism and Culture Ministry of Turkey, the oldest ruins of castle of Asar Hill should be possibly belonging to Mabolla Castle that was mentioned in Hittite texts; open-air sanctuary represents the Hittite's at two thousand years BC and Phrygian and the Urartian traditions at one thousand years ago BC in Karia and Lycian Region (http://www.muglakulturturizm.gov.tr/TR,73784/mugla.html). Moreover, flat top of hill is supplying very good scene of Mugla. Thus, this region is very attractive for natives, domestic and foreign tourists.

Asar Hill contains low-density, medium-porous, and strong Upper Miocene conglomerates packages at the top, and medium-density, low-porous, and very soft fine-grained sediments at the bottom. The flat top of hill contains artificially cut, smoothened, polished, and terraced structure belong to ancient times. Moreover, joints and bedding, seismic activities, and climatic condition of the area promote the physical weathering and break into the blocks of upper most part of conglomerates. Fallen blocks in different size on skirts of Asar Hill, inclined beds, and paleolandslide (SW side of hill) were reported in Asar Hill (Gül et al. 2013). However, they are not studied in detail. Residents are living in old Mugla houses in S-SE of Asar Hill, and many fruit orchards are located in SW of hill (Fig. 1). The climbing route to top of hill is located in SW part of hill. Top of the hill includes some detached blocks (some of them contain ancient stairs and regularly cut and polished towers edge). Possible rock fall hazard is carrying risk for those residents and visitors. So, in situ preservation of blocks including archaeological remnants is of vital importance for tourism and protection of the city historical records. So, research on the lithological and engineering properties of conglomerate, determination of the risky areas around Asar Hill, discussion of the rock fall hazard potential, and possible prevention suggestions are the main aims and impacts of this study.

General geologic setting

The study area mainly contains three different lithologic units namely Gereme Formation, Yatagan Formation, Quaternary alluviums and colluviums (Konak et al. 1987; Göktaş 1998; Gül 2015). Liassic grey-coloured, fractured limestones of the Gereme Formation form rocky mountain around the Mugla Polje (Fig. 2). Relatively flat-top topographies on the Gereme Formation and other older formations are formed by the Yatagan Formation. This formation crops out in the northern part of Mugla city centre (Figs. 1, 2). It also formed Asar Hill, which is the subject of this study. The Yatagan Formation (Upper Miocene, Konak et al. 1987; Aktimur et al. 1996; Göktaş 1998) overlies the older units with angular unconformity, while it is unconformably overlain by the Quaternary deposits including alluvial deposits, colluvial and alluvial fan deposits (Fig. 2). The Yatagan Formation starts with medium- to thin-bedded white marl and claystone (locally crop out) and then continues with thickly bedded red-coloured claystone, siltstone, and lesser extent sandstone (Gül et al. 2013). The fine-grained sediments are overlain by thickly bedded conglomerate packages. The conglomerate packages (totally 140 m thick) are formed by poorly to moderately sorted, crudely imbricated, matrix to clast-supported conglomerates that bear well-rounded Gereme Formation limestone fragments (Gül et al. 2013; Gül 2015). The matrix of conglomerates consists of red–yellow-coloured silt–clay-size sediments. The thin sections of conglomerate and siltstone also include limestone fragments (Gül et al. 2013). Small active and paleolandslides (NE of Asar Hill) were reported in finer-grained sediments of this formation, while rock fall (skirt of Asar Hill) and big karstic caves (SE of Asar Hill) were reported in conglomeratic parts (Gül et al. 2013). NW–SE trending normal active faults cut the Yatagan Formation (Fig. 2). They have


A)
B)
ASAR HILL
BLACK SEA
Ankara
TURKEY
AEGEAN SEA
MEDITERRANEAN SEA
Muğla
1 km
Google earth
Image © 2015 CNES / Astrium

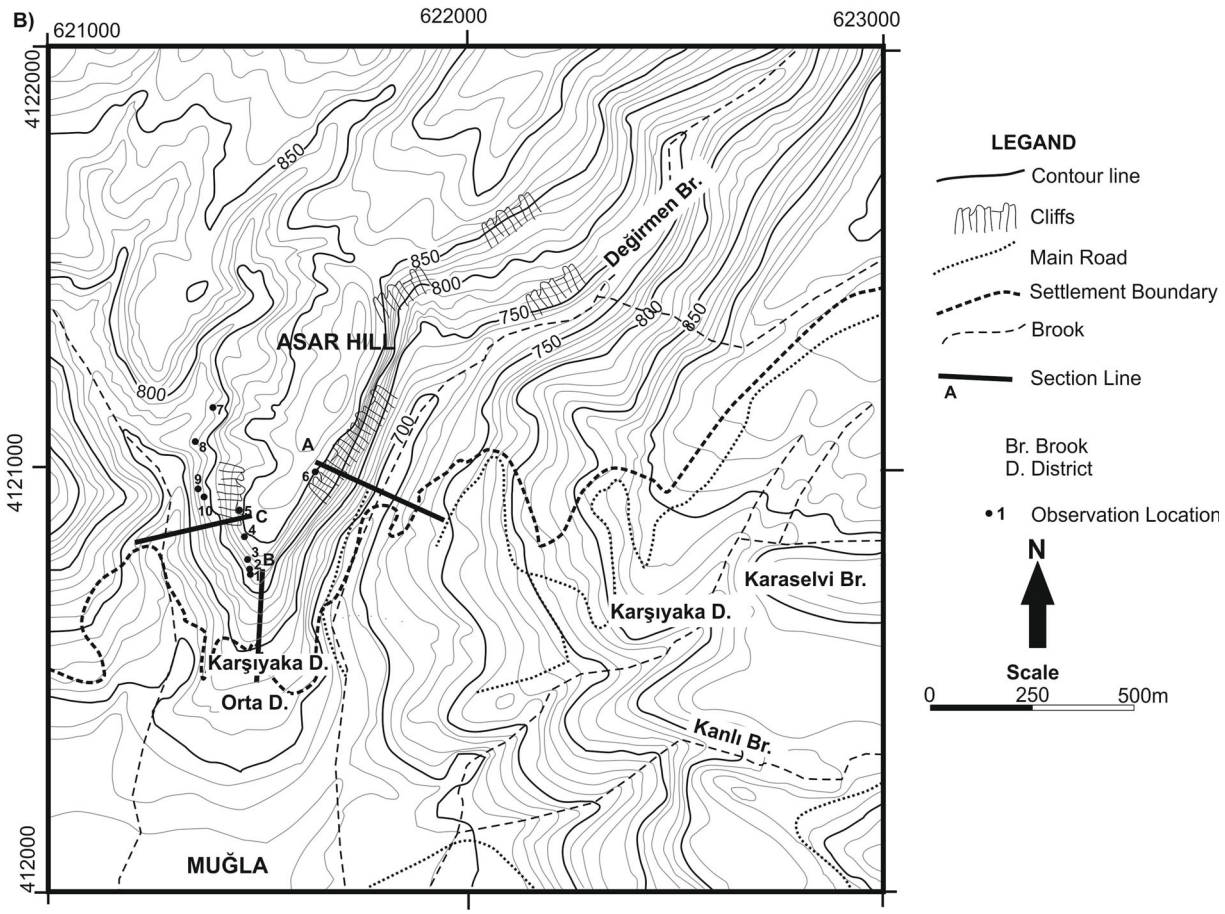
B)
621000
622000
623000
4122000
4121000
412000
ASAR HILL
Değirmen Br.
Karaselvi Br.
Karşıyaka D.
Karşıyaka D.
Orta D.
Kanlı Br.
MUĞLA
LEGAND
Contour line
Cliffs
Main Road
Settlement Boundary
Brook
Section Line
Br. Brook
D. District
Observation Location
N
Scale
0 250 500m

◀**Fig. 1** **a** Field view of the Asar Hill and surrounding region. Fallen blocks are observed at the south–east–west margins of hill. **b** Contour maps of Asar Hill, eastern and western margins are formed by steep-rocky slopes. Three profiles have been taken into consideration during the field and laboratory studies

caused extensive fracture and crack growth at top of conglomerates. Mugla city centre and surrounding region are seismically active zone. Sezer (2003) reported many historical earthquakes in Rhodes Island (7.2 Ms at BC 211; 7.0 Ms at BC 197; 7.0 Ms at BC 183) and Bodrum (8.4 at AD 1886), and 767 earthquakes (Ms $\geq$ 4) were reported in between 1900 and 2000. These active faults and karstic cave collapse in older formation create 3–4 Ms earthquakes every month (Gül et al. 2013). The colluviums were deposited in front of the Gereme Formation and Yatagan Formation Hill, consist of angular–subangular, and poorly sorted breccia (Gül 2015).

Materials and methods

The study area covers roughly 0.12-km^2 flat top of the hill, which is approximately 670 m in length and 170 m in width (Fig. 1). The height of hill is around 880 m (from sea level). The annual temperatures of Mugla range from −11.0 to 42.1 °C (64 years average; MGM 2015a). The annual average rainfall in and around Mugla is 1159.2 mm (64 years average; MGM 2015b). The slope around the hill contains maquis.

Methods used in this study are summarized in Table 1. Field studies were performed in two stages. Three profile lines were selected from the slope of Asar hill in different directions as a result of the general field study (Fig. 1). Structures were scanned and measured along each profile line; bed attitudes were also recorded. Detail field survey was done at the top of the hill during the second stage of field study. Structures and bed attitudes of detached blocks were recorded from different parts of the hill. Persistence, aperture width, nature of filling, termination water flow, and surface roughness of discontinuities were determined based on ISRM (2007). Block size of detached blocks was recorded. Hand samples were collected for laboratory test. Proceq Silver Schmidt Concrete Test Hammer PC Type L' was applied to the grains and matrix of conglomerate and siltstone at the bottom of hill for determining the strength of rock.

Dry-saturate density and porosity tests were carried in the Mining-Geological Engineering Department, Natural Stone Research Laboratory and Rock Mechanic Laboratory

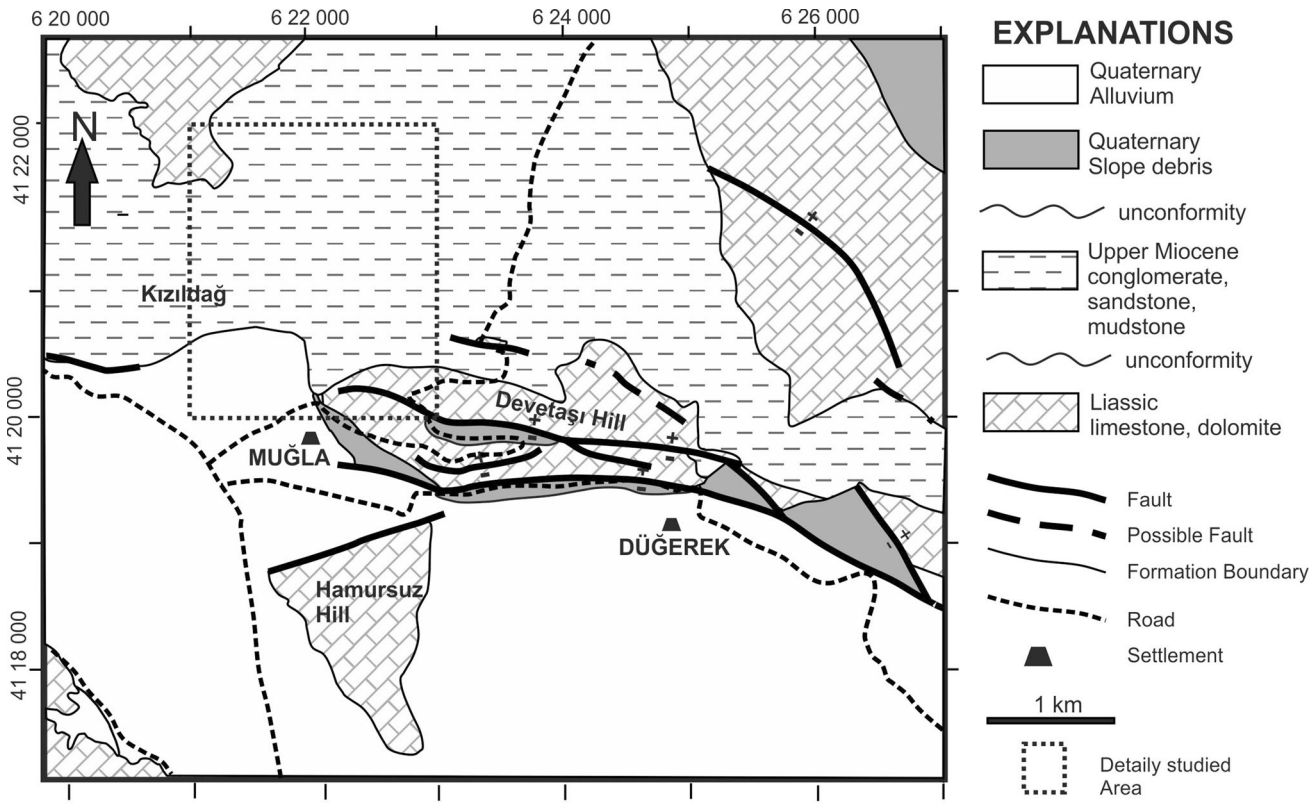

Fig. 2 General geology map of the study area (modified from Konak et al. 1987; Göktaş 1998; MTA 2002; Gül et al. 2013; Gül 2015). Asar Hill is formed by the Upper Miocene conglomerate, sandstone, and mudstone

Table 1 Methods are following during this study

Stage of study	Works
Field studies	First stage,
	Structures and bed attitudes measurement along the profiles
	Second stage
	Structures and bed attitudes measurement of detached blocks
	Block size measurement of detached blocks
	Sample collection for laboratory studies
	Schmidt Hammer application to grains and metric of conglomerate and siltstone
Laboratory studies	Dry-saturate density tests
	Porosity measurement
	Discontinuity analyses using DIPS program
	Rock fall assessment using RocFall version 4.9 software program

of Mugla Sitki Kocman University. Discontinuity analyses were carried out using DIPS program, and dominant joint sets were determined. RocFall version 4.9 software program (Rocscience 2002; Yılmaz et al. 2008) was used to analyse the possible rock fall characteristic of detached blocks on top of the Asar Hill. RocFall version 4.9 software program statistically analyses rock mass movement based on lumped mass method, which assume that blocks move along the single trajectory in profile (Rocscience 2002). The program is also used to analyse bounce height, velocity, run-out distance, and kinetic energy.

Results and discussion

Physical and mechanical properties

The conglomerate samples were taken from the top of Asar Hill, while siltstone samples were taken from the bottom of hill. The average dry density of conglomerate is 1.9 g/cm^3, and porosity ratio is 6.4 %. Average dry density of siltstone is 2.5 g/cm^3, and porosity ratio of it is 4.0 % (Table 2). The conglomerate is classified as a 'low density rock and medium porous rock' according to (Anon 1979). The siltstone is classified as a 'medium density rock and low porous' rock according to (Anon 1979).

Schmidt hammer rebound values

The rebound values of conglomerate have been fixed via direct application to the grains (embedded in the matrix, grain cover area >7 cm^2) and matrix (Table 3). Grain denoted results of Schmidt Hammer application perpendicular to grain surface, and matrix indicates application results of Schmidt Hammer to binding materials of conglomerate. Grain-1 and Grain-2 measurements were taken in Profile B area; Grain-3 and Grain-4 and matrices measurements were taken in Profile A region. According to De Beer (1967) classification, matrix of conglomerate is in 'soft rock' class, while grains are in 'very strong rock' class. Overall the matrix should weaken the grains; thus, the conglomerate can be evaluated as a 'strong rock' class (De Beer 1967). The siltstone is evaluated as a 'very soft rock' based on De Beer (1967) classification. The moist rock condition, which should decrease the in situ rock strength, was fixed in siltstone close to Schmidt Hammer impact point.

Kinematic analysis

Dip and dip directions, and engineering properties of joints were scanned and measured along the A, B, and C profiles lines (Fig. 1; Table 4). Contour diagrams of joints were drawn using the DIPS 6.0 software program, and dominant joint sets were determined (Diederichs and Hoek 1989; Rocscience 2015) (Fig. 3). Profile A line contains single joint set and randomly distributed joints. Profile B includes three joint sets, and Profile C consists of four dominant joint sets and randomly distributed joints (Fig. 3; Table 4). The joints persistences vary between 'very low persistence (<1 m) and high persistence' (10–20 m; ISRM, 2007). Joint terminations are both ends visible. Aperture width varies between 'wide (>10 mm) and extremely wide' (10–100 cm; ISRM 2007). Clay-size sediments, as matrix of conglomerate, are filling the joints. Rough joints have planar and undulatory surface shape. The spacing of them ranges between 'wide spacing (600–2000 mm) and very wide spacing' (2000–6000 mm; ISRM 2007). Water infiltration is observed at the bottom of conglomerates where the contact with siltstone. The dipping of Yatagan Formation is towards the NW, and dip angle varies between 20° and 35°. The bedding surfaces also act as weakness zone and increase the discontinuity effect when crossing with the other discontinuities.

Kinematic analyses can be carried out before the detailed failure analyses (Akbulut 2012). Planar sliding,

Table 2 Dry-saturated density, dry-saturated unit weight, and porosity values of conglomerate and siltstone

	Dry density (g/cm^3)	Dry unit weight (kN/m^3)	Saturated density (g/cm^3)	Saturated unit weight (kN/m^3)	Porosity (%)
Conglomerate					
n (number of experiment)	5				
Max	2.1	20.7	2.2	21.6	9.7
Min	1.5	14.7	1.6	15.4	3.5
Average	1.9	18.5	2.0	19.2	6.4
STD	0.23	2.29	0.24	2.33	2.62
Siltstone					
n (number of experiment)	2				
Max	2.7	26.5	2.7	26.9	4.3
Min	2.4	23.5	2.4	23.9	3.7
Average	2.5	25.0	2.6	25.4	4.0
STD	0.21	2.09	0.22	2.13	0.42

Table 3 Rebound values of grains and matrix of conglomerate and siltstone

	Conglomerate						Siltstone
	Grains-1	Grains-2	Grains-3	Grains-4	Matrix-3a	Matrix-4a	
Application direction	1	3	3	3	3	3	3
Rebound values	50.6	44.1	51.2	46.2	32.3	22.8	21.1
Average	48.0				27.6		

1: perpendicular to bedding; 3: parallel to bedding

Table 4 Parameters used in kinematic analyses

Profiles	Slope attitude (dip/dip direction)	Dominant joint set	Internal friction angle of joint sets
A	80°/115°	73°/179°	37°
B	80°/172°	71°/334°, 67°/174°, 74°/149°	37°
C	80°/257°	60°/160°, 72°/197°, 72°/8°, 74/°331°	37°

flexural toppling, and wedge-type failure are examined based on internal friction angles, attitudes of joints and slopes. Friction angle of conglomerates varies between 34° and 40° (Wyllie and Mah 2004). Moreover, RocLab also pointed out the approximately 37° based on an assumptions (specimen requires more than one blow of a geological hammer to fracture, and Geological Strength Index is assumed as a 50 based very blocky and fair surface condition). Thus, it was taking as 37° in these kinematic analyses.

There is no big risk in Profile A in terms of planar sliding, wedge-type failure, or flexural toppling (Fig. 3). In Profile B, planar sliding and flexural toppling are generally controlled by the 71°/334° joint set, crossing of 71°/334° and 67°/274° with 67°/274° and 74°/249° cause wedge-type failure (Fig. 3). In Profile C, crossing of 72°/197° joint set with 74°/331° joint set controls the wedge-type failure (Fig. 3).

RocFall software application

RocFall software is used for assessment of the potential rock fall hazard. Friction angle is one of the required values for programme, calculated as a 37° ± 3° based on RocLab applications. The surface is taken as clean hard rock. Surface roughness is taken as a 2 as proposed for similar application (Topal et al. 2012). Some ways for estimation of *Rn* and *Rt* restitution coefficient values summarized in program help section based on previous studies (Rocscience 2002), or can be determined with laboratory application and back analysis (Chau et al. 2002; Topal et al. 2006, 2012; Binal and Ercanoğlu 2010; Asteriou et al. 2012). Peng (2000) and Richards et al. (2001) have proposed successive formulas for (Rn) values of different rocks. N1 and N2 are Schmidt Hammer Rebound Values for laboratory and slab samples. We obtained them from average values of grains and matrix. From these, *Rn* values and *Rt* values were obtained from back analysis in A profile (slope 45°; Fig. 4).

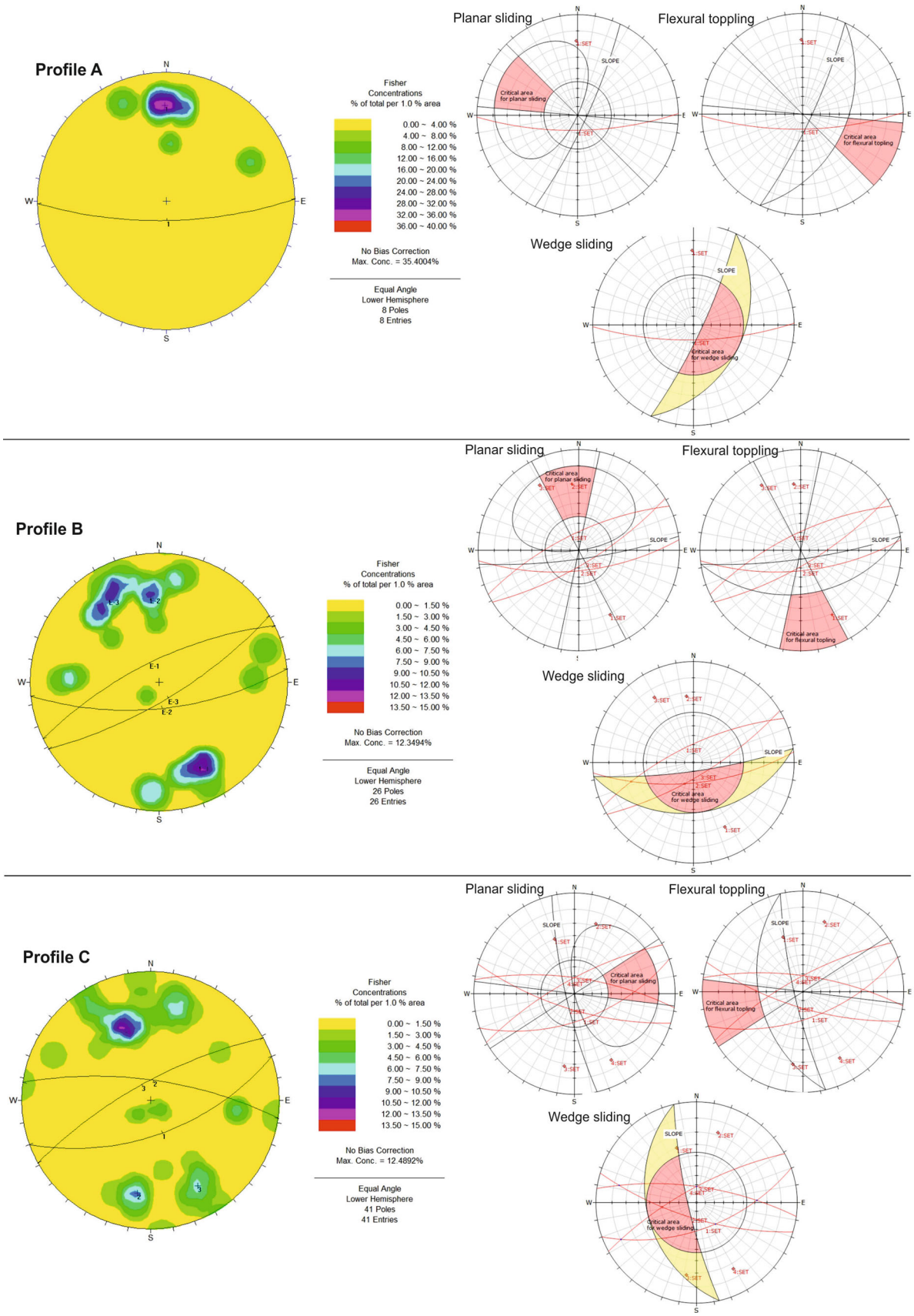

Fig. 3 Kinematic analyses results based on DIPS application

Fig. 4 **a** The fortification wall block includes stairs. This detached block is just sitting at the edge of cliff (Man for scale 1.73 m). **b** Another fortification wall block is detached from main hill. Only small earth fill part is located between these two blocks (Bag for scale 36 cm width). **c** General view of the Profile A. **d** Fallen blocks, located at the bottom of the Profile A, used for back analysis in RocFall application

$$
\begin{aligned}
Rn &= -0.110 + 0.00919 * \mathrm{N1} + 0.00392 * \mathrm{N2} + 0.00358 * \mathrm{A} \\
Rn_{\mathrm{graincong}} &= -0.110 + 0.00919 * 48 + 0.00392 * 48 + 0.00358 * 45 \\
Rn_{\mathrm{graincong}} &= 0.68 \\
Rn_{\mathrm{matrixcong}} &= -0.110 + 0.00919 * 27.6 + 0.00392 * 27.6 + 0.00358 * 45 \\
Rn_{\mathrm{matrixcong}} &= 0.41
\end{aligned}
\tag{1}
$$

So *Rn* values between the 0.40 and 0.9 were taken into consideration in back analysis (Fig. 5). The back analysis was done for five different blocks (350, 832, 2860, 4560, and 12960 kg). The end points of blocks after 1000 throws were taken into consideration. Most of fallen blocks were dispersed in valley in between 180 and 242 m of Profile A (Figs. 4, 6a). Thus, the highest throws in that part were researched during the back analysis using different *Rn* and *Rt* values as proposed by different researchers (Chau et al. 2002; Topal et al. 2006; Binal and Ercanoğlu 2010; Asteriou et al. 2012). This graph also includes the soil slopes and rock slopes boundary according to different researchers (Fig. 5; Wu 1985; Fornaro et al. 1990). *Rn* 0.7 ± 0.05 and *Rt* 0.85 ± 0.05 values were fixed for further process of RocFall application in our study. They are roughly at the midpoint of rectangular region pointing the average values of our data (Fig. 5). Similarly Topal et al. (2012) used a rectangular area obtained after omitting lower and higher values; the centre of rectangular area was taken as a representative values. Table 5 shows RocFall parameters that used in this study.

Three profiles were selected based on detached conglomerate blocks. Profile A is situated on the eastern skirt, Profile B southern skirt, and Profile C on south-western skirt of Asar Hill (Fig. 1). All of those profiles start with nearly 5–10-m-high rocky, cliff part and then pass into inclined part of the hill (Figs. 4, 6, 7, 8).

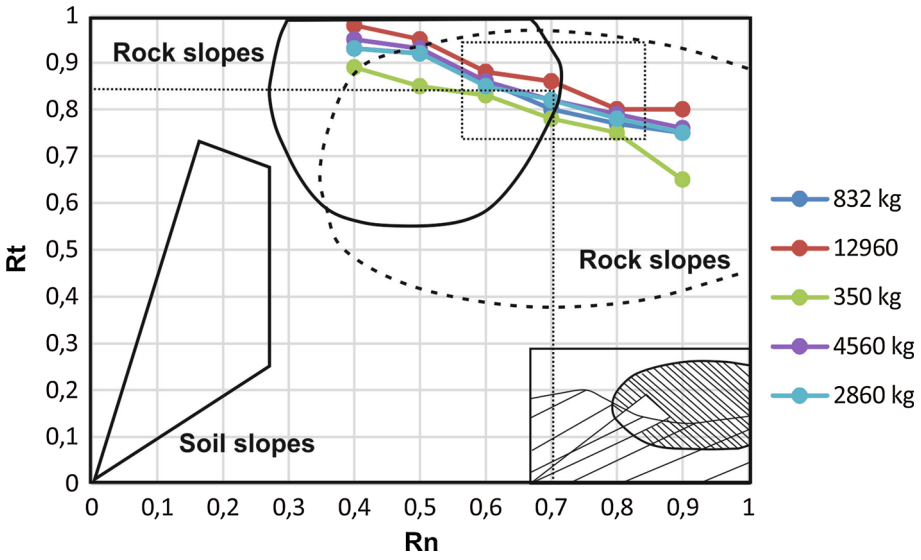

Fig. 5 Rn versus Rt graphs obtained as a result of back analysis in the study area. The *graph* is also including soil slope (Wu 1985) and rock slope limit (Wu 1985; *dashed line* proposed by Fornaro et al. 1990) data of different researcher. *Rectangular with dotted line* represents the average values for this study. Average *Rn* and *Rt* is also marked for further process

Profile A

The Profile A contains 2 separated blocks; first and the most dangerous rectangular prism one (detached block) is located at the edge of hill, and the dimensions of it 220 (length) × 290 (width) × 100 (height) cm, but 100 × 70 × 120 cm size of stairs rectangular prism space were extracted from total volume. The saturated weight of this block is 11.080 tonnes (11080 kg, Fig. 4a). Second block, located between the first detached block and hill, may fall after falling of the first block. The dimensions of this rectangular prism block are 570 × 450 × 410 cm and contain cut space 210 × 300 × 80 cm in dimensions that extracted from total volume. The saturated weight of this block is 200.25 tonnes (200250 kg; Fig. 4b). Those blocks have a great risk to fall down (Fig. 4c) and may join to other fallen blocks at the bottom of the Profile A (Fig. 4d). RocFall application indicated that two reached blocks trajectories may end at around the 200 m in the middle of valley (Fig. 6a; Table 6). The average bounce height of those blocks is around 11.5 m, and translational velocities have close values 21–22 m/s. However, kinetic energies of blocks are variable depend on their mass difference.

The Profile A has the highest slope of all three profiles (Fig. 6). Thus, the highest bounce height and translational velocity are observed in this profile (Table 6). According to RocFall results, some blocks passed to other side of the valley that includes some houses. Possible down valley movement of block after falling may take into consideration in further assessment. The bedding plane inclined through interior of Asar Hill (opposite of slope). Wedge-type failure is determined based on kinematic analysis (Fig. 3). However, toppling of blocks can be viewed at the beginning of movement depend on cliff surface; then, bouncing and rolling may observed through the lower part of profile. Both examined blocks contain archaeological traces (cut–polished–shaped surface and stairs); thus, in situ conservation of the blocks is of vital importance.

Profile B

The Profile B is of medium slope than other profiles (Figs. 1, 6b, 7a). This profile includes two detached blocks; their upper surface is in elliptical shape. The first block is separated from host rock mass via 1-m-wide crack that may widen depend on continuous water action, weathering, and/or seismic activities. The '*a*' and '*b*' axes of that ellipsoidal top block are 775 and 255 cm, respectively, and the height of this block is roughly 1000 cm. The '*a*' and '*b*' axes of second block are 460 × 265 cm, and height of it is roughly 900 cm. The first block weight is calculated as 1241.085 tonnes (1241085 kg; Figs. 6b, 7b), and the second block weight is calculated as a 688.9788 tonnes (688978.8 kg). Only the Profile B contains one or two floors houses at the bottom that added as a barrier in profile section (Figs. 6b, 7a). The blocks of Profile B are the largest block of the study area. RocFall application results indicate that those blocks are not reaching to the end of profile. They may stop in the middle of profile (Fig. 6b). The average end point of the blocks is around 81–82-m horizontal distance (Table 7). The bounce height, kinetic energy, and translational velocity are presented in Table 7. Huge mass of second block is preventing the measurement of bounce height, kinetic energy, and translational velocity due to rolling-sliding of block (Table 7).

As a result of the field studies, the largest blocks were found in the Profile B, while the lowest angle of slope was also observed in this profile (Figs. 6b, 7; Table 7). Thus, blocks should only move to the middle of profile (Figs. 6b, 7). Bounce height, total kinetic energy, and translational

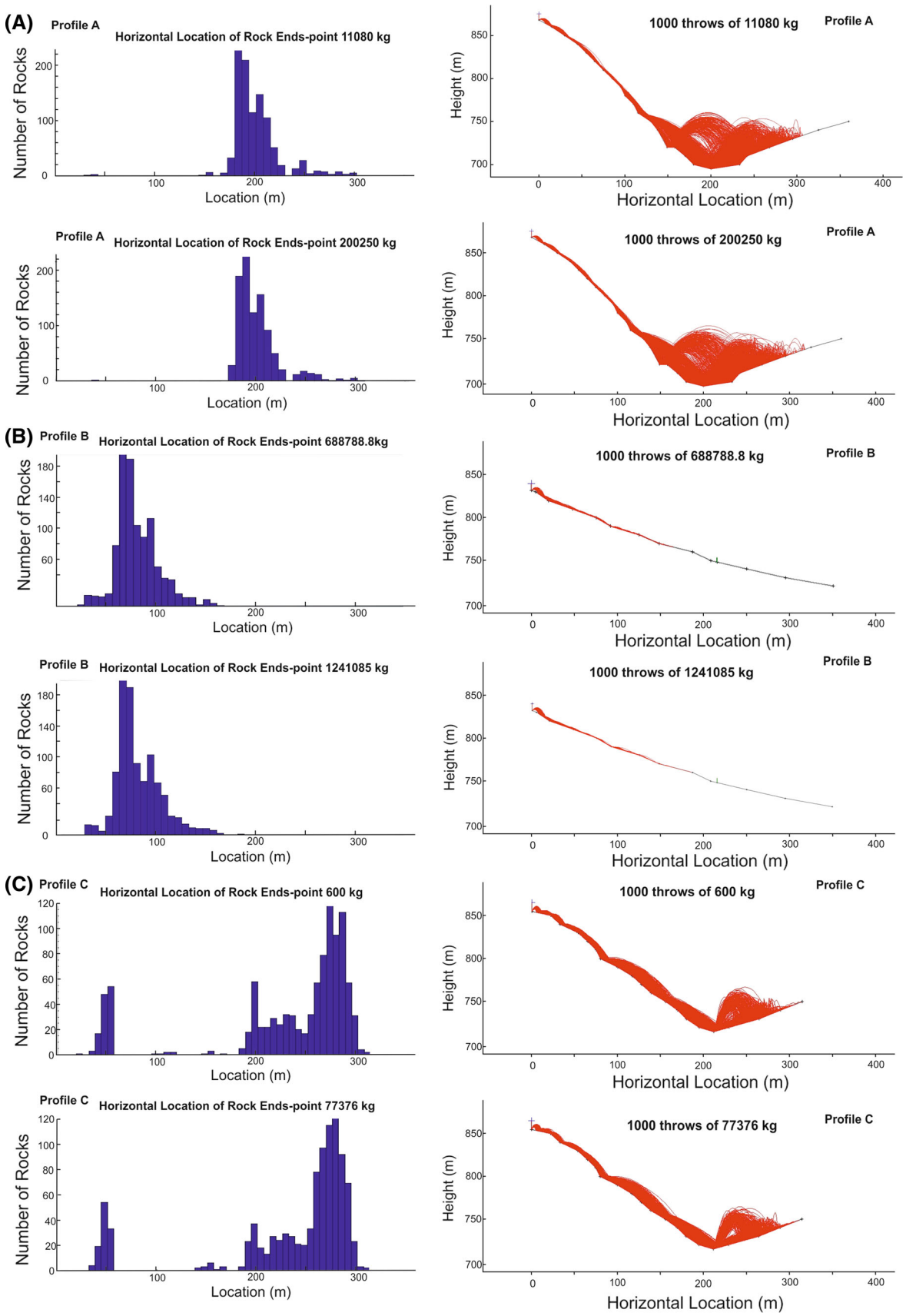
(A)
Profile A
Horizontal Location of Rock Ends-point 11080 kg
Number of Rocks
Location (m)
1000 throws of 11080 kg
Profile A
Height (m)
Horizontal Location (m)
Profile A
Horizontal Location of Rock Ends-point 200250 kg
Number of Rocks
Location (m)
1000 throws of 200250 kg
Profile A
Height (m)
Horizontal Location (m)
(B)
Profile B
Horizontal Location of Rock Ends-point 688788.8kg
Number of Rocks
Location (m)
1000 throws of 688788.8 kg
Profile B
Height (m)
Horizontal Location (m)
Profile B
Horizontal Location of Rock Ends-point 1241085 kg
Number of Rocks
Location (m)
1000 throws of 1241085 kg
Profile B
Height (m)
Horizontal Location (m)
(C)
Profile C
Horizontal Location of Rock Ends-point 600 kg
Number of Rocks
Location (m)
1000 throws of 600 kg
Profile C
Height (m)
Horizontal Location (m)
Profile C
Horizontal Location of Rock Ends-point 77376 kg
Number of Rocks
Location (m)
1000 throws of 77376 kg
Profile C
Height (m)
Horizontal Location (m)

◀**Fig. 6** Horizontal location of rock end points and profile-throw trajectories are presented separately for each profiles. **a** RocFall applied for 11080 and 200250 kg blocks in Profile A. The valley located at the skirts of profile prevents further movement of the blocks. **b** RocFall applied for 688788.8 and 1241085 kg blocks in Profile B. The barrier is only added to this profile, because one- or two-floor houses are located in the skirt of this profile. **c** RocFall applied for 600 and 77376 kg blocks in Profile C. The valley at the bottom of profile includes some small gardens

Table 5 RocFall application parameters

Coefficients	Values
Rn	0.7 ± 0.05
Rt	0.85 ± 0.05
Throw	1000
Friction angle	37° ± 3°
Surface roughness	2
Surface of slope	Clean hard rock

velocity cannot be calculated by the software program due to huge mass (Table 7). Wedge-type failure is dominant failure type based on kinematic analysis (Fig. 3). After the initial falling and toppling, those blocks may slide along the profile and may stop before the pine forest and houses. Thus, they are not carrying risk for houses, while one–two-floored houses situated at the top of the enlarging karstic caves. Possible collapse of those caves may threaten the houses and residents.

Profile C

The Profile C is located in rocky and cliff western side of Asar Hill (Figs. 1, 6c, 8a). Crossing of joints and bedding planes led to formation of several blocks with varying size and mass at the top of Profile C (Fig. 8b). Termination of joints caused the different shaped blocks. Weights of rectangular prism blocks, 390 × 310 × 320 cm, 50 × 60 × 100 cm, and 150 × 150 × 150 cm, are 77.376 tonnes (77376 kg), 0.6 tonnes (600 kg), and 6.75 tonnes (6750 kg), respectively. Some blocks have an ellipsoidal geometry in plan view, their '*a*', '*b*' axes and heights are 250 × 125 × 270 cm, 80 × 200 × 280 cm and 155 × 205 × 170 cm, and their weights are 52.9875 tonnes (52987.5 kg), 28.1344 tonnes (28134.4 kg) and 33.92299 tonnes (33922.99 kg), respectively. RocFall program results of those blocks are presented in Table 8, while only the largest and the smallest block views are presented in Fig. 6c. The average horizontal rock ends points are ranging from 231 to 237 m (Table 8). However, significant amount of rock ends points is concentrated between 270 and 290 m at north-west of valley of Asar Hill (Figs. 1, 6c). The average bounce height of those blocks is 2.64–2.88 m, and translational velocities are 25.15–25.94 m/s (Table 8). The kinetic energies of blocks are highly variable due to mass differences (Table 8).

The Profile C has the second highest slope in examined profiles (Fig. 5). RocFall application results point out that mean horizontal rock end points are located inside the valley; however, significant rocks ends pass to west side of valley (Figs. 1, 6c; Table 8). Three joint sets and randomly distributed joints and bedding caused the excessive fragmentation and formation of many blocks in different size. Wedge-type failure is dominant failure type based on kinematic analysis (Fig. 3). However, toppling and of possibly planar sliding (due to bedding) of blocks can be monitored at top of the profile because of cliff, and then,

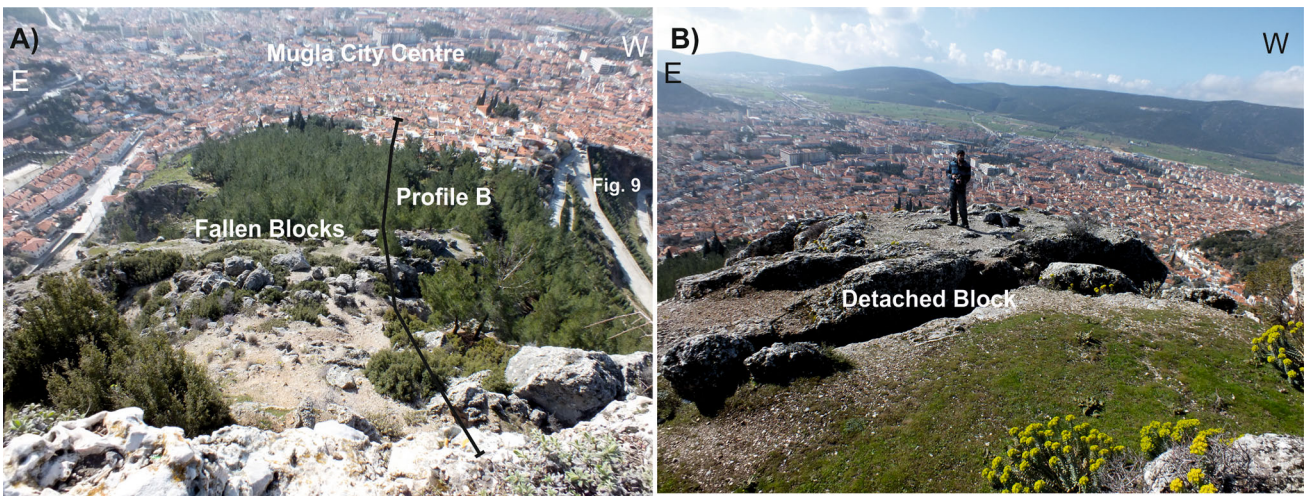

Fig. 7 **a** General field view of the Profile B from top of Asar Hill. The profile is extending to one- or two-floor houses. The middle part of profile contains fallen blocks. Then 5–8-m-high pine forest is observed. **b** Field view of the detached block (688978.8 kg). Nearly 1-m-wide joint is separated the block from the main formation body (man for scale 1.73 m)

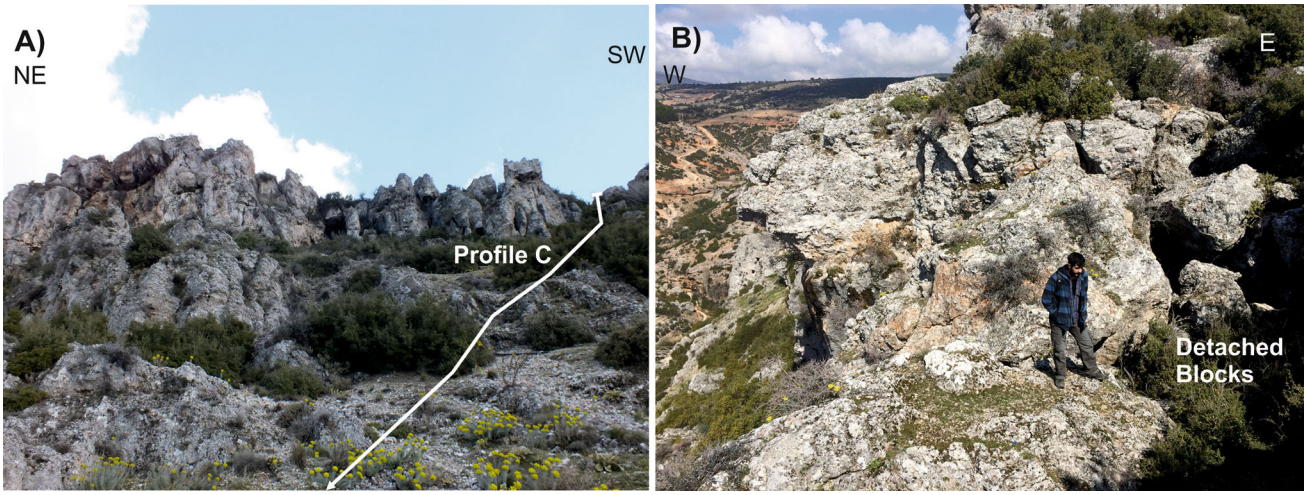

Fig. 8 **a** General field view of the Profile C from the *bottom* to *top* of hill. The *upper* part of profile is totally formed by the conglomerate packages, while the *bottom* part contains sandstone–mudstone, and erosive-based channelized conglomerates. The dipping of beds (NW) has same direction with slope. **b** The crossing of joints and bedding planes have caused fragmentation of the Yatagan formation and led to formation of several blocks

Table 6 Statistical evaluation of the end point, bounce height, total kinetic energy, and translational velocity distribution of two blocks along the A profile

RocFall properties	Horizontal rock end points (m)		Bounce height distribution (m) at 180 m		Total kinetic energy (J) at 180 m		Translational velocity distribution (m/s) at 180 m	
A profile								
Block mass (kg)	11080	200250	11,080	200250	11080	200250	11080	200250
Min	44.67	37.51	0	0	5869.54	73,861.2	0.43	0.69
Max	303.9	316.26	55.47	56.57	1.11E+7	1.94E+8	40.75	40.37
Mean	201.8	200.84	11.78	11.03	4.28E+6	7.83E+7	21.65	21.91
Std	22.14	25.54	14.68	14.07	3.71E+6	6.72E+7	13.57	13.59

Bounce height, total kinetic energy, and translational velocity distribution were taken from mid of profile

Table 7 Statistical evaluation of the end point, bounce height, total kinetic energy, and translational velocity distribution of two blocks along the B profile

RocFall properties	Horizontal rock end points (m)		Bounce height distribution (m) at 170 m		Total kinetic energy (J) at 170 m		Translational velocity distribution (m/s) at 170 m	
B profile								
Block mass (kg)	688978.8	1241085	688978.8	1241085	688978.8	1241085	688978.8	1241085
Min	30.97	25.89	0	0	8.55E+6	0	3.82	0
Max.	186.53	166.04	0.02	0	5.74E+7	0	11.16	0
Mean	82.22	79.94	0	0	3.50E+7	0	7.87	0
Std	22.52	20.93	0.01	0	2.38E+7	0	3.37	0

Bounce height, total kinetic energy, and translational velocity distribution were taken from mid of profile

bouncing and rolling may observed through the lower part of profile. The highest possible rock fall should observe in this area due to excess block formation. Moreover, the bedding of conglomerates and slope of hill are in the same direction, inclined to NW that increases the possible rock movement along the Profile C. This profile also cut Asar Hill climbing lane; in addition, many gardens are located in the bottom valley. So, the most human activity is observed in this region. Consequently, the possible rock fall of Asar Hill is carrying the highest risk for people in this region.

Table 8 Statistical evaluation of the end point, bounce height, total kinetic energy, and translational velocity distribution of six blocks along the C profile

RocFall properties	Horizontal rock end points (m)					Bounce height distribution (m) at 157.5 m					
C profile											
Block mass (kg)	600	6750	28134.4	33922.99	52987.5	77376	600	6750	28134.4	33922.99	52987.5	77,376
Min	34.77	37.45	36.77	34.44	36.87	37.89	0	0	0	0	0	0
Max.	310.05	315	311.06	315	315	315	17.49	15.62	16.04	21.11	17.26	19.82
Mean	236.46	231.3	232.83	231.72	231.71	231.23	2.75	2.77	2.88	2.59	2.64	2.78
Std	70.48	76.80	72.35	74.93	75.86	73.63	2.51	2.52	2.54	2.45	2.34	2.56
RocFall properties	Total kinetic energy (J) at 157.5 m						Translational velocity distribution (m/s) at 157.5 m					
Block mass (kg)	600	6750	28134.4	33922.99	52987.5	77376	600	6750	28134.4	33922.99	52987.5	77,376
Min	2001.12	7145.6	149,121	156,463	94,317.2	72,598.9	2.14	0.65	2.58	2.51	1.34	0.71
Max.	509,129	5.58E+6	2.38E+7	2.75E+7	4.55E+7	6.48E+7	38.86	38.26	38.71	38.24	38.99	38.69
Mean	260,080	2.99E+6	1.25E+7	1.44E+7	2.29E+7	3.29E+7	25.42	25.76	25.94	25.19	25.46	25.15
Std	92,403.9	1.02E+6	4.15E+6	5.10E+6	7.53E+6	1.14E+7	5.90	5.75	5.40	5.60	5.27	5.74

Bounce height, total kinetic energy, and translational velocity distribution were taken from mid of profile

Karstic caves

The big caves are located at the bottom part of Profile B. The caves are observed inside of the conglomeratic packages on top of the red-coloured sandstones–mudstones. The fine-grained parts are wet and contain water leakages. The conglomerate has higher porosity than this fine-grained part. Thus, groundwater may largely active at the boundary of conglomerate and fine-grained sediments. The weakening and washing of matrix (moreover lower strength of matrix) release of grains of conglomerate. Removing of grains and dissolution of the limy parts of Yatagan Formation led to formation of big caverns. One- or two-floor houses, at the top of these caverns, are under threat of those caves collapse (Fig. 9) because enlargening of caves depends on water action and weathering. So overburden thicknesses of caves are continuously decreasing.

Mass-wasting movements have significant effect on geomorphology, natural hazards to life and property, and civilization (Hermanns et al. 2006; Ocakoglu et al. 2009; Topal et al. 2012; Alemdag et al. 2014; Tang et al. 2014). Rock fall, observed in Asar Hill, is one of the examples of rapid mass movement (Varnes 1978; Hungr et al. 2014). Several different reasons including the lithological properties, climatic conditions, seismicity, structural properties, human effects, and different weathering may control mass movement characteristic (Wasowski and Gaudio 2000; Agliardi and Crosta 2003; Frayssines and Hantz 2006, 2009; Topal et al. 2012; Wei et al. 2014). Sometimes one or two factors come forward. For example, heterogeneity, structural properties, and steep slopes control the rock fall in Al-Hada Mountain in Saudi Arabia (Sadagah 2015). Seismic activity and structural properties control the rock fall in Monemvasia historical site located in Peloponnese in Southern Greece (Saroglou et al. 2012). Typhoon in northern Taiwan in 2013 caused the rock fall disaster (Wei et al. 2014). Frayssines and Hantz (2006) reported that rock falls in Subalpine Ranges (French Alps) have strong correlation with freeze-thawing cycles, slight correlation with rainfall, and no correlation with seismic activities. Alejano et al. (2013) reported that raining and lesser extent freezing are determined as main triggering factors for rock fall in limy conglomerate canyon in Covarrubias—Burgos in northern Spain.

Similarly, rock fall assessment can change depending on rock type, location, and researchers experience. For example, Hermanns et al. (2006) used geomorphological features, aerial photographs, shaded image relief, seismic reflection profile, and finite element analysis rock avalanches in Austria and Norway. Frayssines and Hantz (2006) worked on the 25 rock falls using time relation, structural properties, and climatic condition in French Alps. RocFall program was also used for assessment of

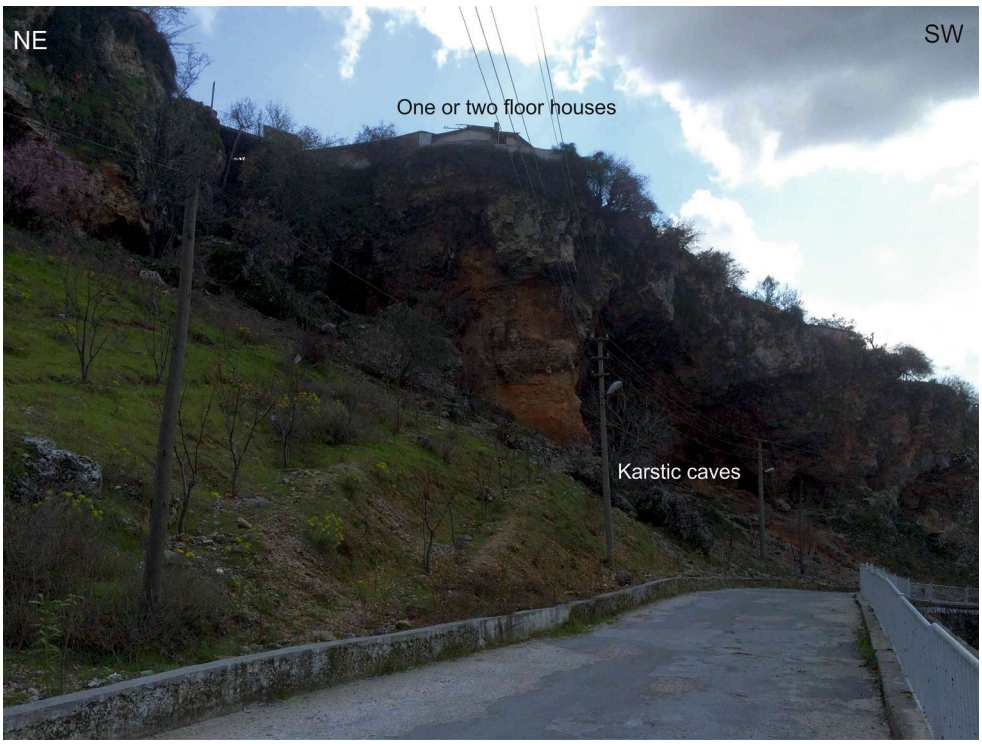

Fig. 9 Weakening of mud matrix due to groundwater and partially surface water, then washing of matrix of the conglomerate led to disintegration of grains and formation of big karstic caves inside the formation (fence for scale 1.5 m). One- or two-floor houses are located at the *top* of caves

rock fall hazard in Marun Dam in SW Iran (Koleini and Van Rooy 2011), for estimation of measures for possible rock fall at the historical site of Monemvasia, Greece (Saroglou et al. 2012), for zoning map and rock fall assessment in Erzincan, Turkey (Keskin 2013) and for evaluation rock fall assessment in flysch deposit in Kuşadası, Turkey (Kaya and Topal 2015).

The crossing of joint sets and bedding are responsible from initial fragmentation of the Yatagan Formation conglomerate in Asar Hill. Persistences of joints control the block size. Bedding controls the slope of Asar Hill. Subsequently seasonal and daily temperature differences, intense seasonal raining especially during winter and spring terms, high seismic activity, gravity, strength differences of grains and matrix of conglomerates and both surface and groundwater circulation promote the weathering effect and block formation on top of Asar Hill. Then those blocks are moved downdip due to gravity effect and/or shaking of ground. The detached blocks at top of Asar hill route were analysed using RocFall program according to data obtained from back analysis of previously fallen blocks. During this study (even during review process of paper), the detached block monitored, they are not falling. However, the gap between those blocks and main body of hill are widened. Moreover, some small rock falls detected around hill; their end locations are consistent with the RocFall program results. Most of those blocks especially on road were cleared immediately by municipality. According to archaeological information, Asar Hill had been also shaped by human activities since 2000 years ago BC. Humans had cut, smoothened, shaped, carved, and terraced top of the Asar Hill, and western side of the hill. Thus, the humans created additional weathering surface and weaken the rock indirectly.

Different remediation techniques can be suggested for preventing undesirable effects of mass movements. Sadagah (2015) emphasized endangers due to engineering application without taking any support. He also suggested that back analysis can show the location of seed points, and modelling of rock fall barriers must be prepared before the artificial slope creation. Topal et al. (2006) suggested that cleaning of loose blocks, then bolting and protective fences for prevention of rock fall hazard zone for Afyon Castle on top of the volcanic rocks. Topal et al. (2012) proposed that rock bolts application at lower levels of the hill after cleaning the loose blocks, in addition 2–4-m-high fences with a maximum capacity of 2.600 kJ recommended to stop rock fall nearby settlement area for Kastamonu Castle. Zorlu et al. (2011) suggested that the application of preventive methods for rock fall in Cappadocia region—Turkey—including trenching, bolting, low barriers, and netting for safe tourism even though no settlement. Saroglou et al. (2012) suggested that two different support measures to prevent rock fall in the Monemvasia historical site in

Southern Greece. Those are an application of external force to the rock face by tensioned rock anchors and/or patterned rock bolts and protective measures from active rock fall such as rock barriers (Saroglou et al. 2012). They suggested tensioned anchors or pattern bolting application for individual huge blocks and spot bolting for smaller blocks at the suitable part of the slope crest. They mentioned that rock fall barriers cannot prevent the blocks heavier than the 10 tonnes; thus, bolts and wire rope applications are necessary in this type movement. Archaeological sites are under the preservation of special legislation, so every support measures such as spray concrete, steel nets cannot freely applied (Saroglou et al. 2012).

The blocks including archaeological material like in Profile A should be attached to main rock body with suitable tensioned rock anchors and/or patterned rock bolts for avoiding rock fall. Their in situ preservation is critically important to keep safe of city history record. The water canal in east of the profile can be widened in order to prevent the passing of rock fall to eastern side of valley. Recently the huge blocks on top of Profile B cannot threaten the peoples, and the mid-slope areas must be kept as a forest area for avoiding from the rock fall hazard. Or initially archaeological remnants are checking, and then, the block size can reduce and clean. Moreover, the size of cavernous structure at the bottom of Profile B (Fig. 9) must be determined and collapse possibility of it must be researched in detail; if necessary, houses on top of caves should be relocated. The western side (Profile C and surrounding) of Asar Hill requires special treatment due to excess human activities. Many domestic and foreign tourist use the western path to climb the top of the hill. The detached blocks must be cleaned and then depend on block size spot-pattern bolting, and tensioned anchors can be applied. Trench application and garden relocation can be considered at the downhill of the Profile C.

The protection from mass movement rock fall sometimes carries vital importance for people. If blocks that carry great risk for rock fall include the archaeological ruins, the in situ protection requirement of ruins is restricted support measures choices. Before the final support measures decision, the scientist and engineers must work together in order to understand the characteristics of mass wasting including size of rock mass, rock fall path and type of mass movement, and controlling factors for local mass movements.

Conclusions

Structural properties of the Upper Miocene Yatagan Formation conglomeratic packages in Asar Hill are the main controlling factors of block formation. Intersection of joint sets and bedding, and persistence of joints control block size. The intersection of them and bedding direction (inside hill direction led to the highest slope) also affect morphology of hill, and mass movement types. Climatic conditions, seismic activities, gravity, strength differences of matrix, and grains of conglomerates increase weathering, formation of block, and initiation of rock fall. Beside these natural effects, the human activities, started roughly 4000 years ago before present, promote weathering surface due to cut, terrace, and carve of rocks. Some blocks at top of hill include archaeological remnants; thus, their in situ preservation has vital importance. Large blocks can be fixed with suitable tensioned rock anchors and/or patterned rock bolts at the hill crest. This application must be done immediately, because two detached blocks on eastern crest of hill contain archaeological ruins. After the archaeological investigations, detached blocks at the top of western crest can be clean or fixed with bolts. This part is situated above the tourist climbing route to top of hill and downhill gardens. The necessary precautions must be taken immediately in this region too. Trench, relocation of houses and garden, and formation of forest-green belt are other recommended precaution methods at the bottom of hill for preventing the people form rock fall hazard and cave collapse.

Acknowledgments The authors thank to Mr. Onur Bozdemir and Mr. Övünç Alca for their helping during the field and laboratory studies. The authors also thank to reviewers, editors, and journal staff for their valuable contributions.

References

Agliardi F, Crosta GB (2003) High resolution three-dimensional numerical modelling of rockfalls. Int J Rock Mech Min Sci 40:455–471

Akbulut İ (2012) Slope stability (Şev Duraylılığı), education series of mineral and research institute of Turkey (Maden Teknik ve Arama Genel Müdürlüğü Eğitim Serisi) no. 42 Ankara, p 160 (**in Turkish**)

Aktimur HT, Sarıaslan MM, Sönmez M, Keçer M, Uysal Ş, Özmutaf M (1996) Field usage potential of Muğla province (Central Town) (Muğla İlinin (Merkez İlçe) Arazi Kullanım Potansiyeli). Mineral and Research Institute of Turkey (Maden Teknik ve Arama Genel Müdürlüğü) report, 9853, p 33 (unpublished, **in Turkish**)

Alejano LR, Garcia-Cortes S, Garcia-Bastante F, Martinez-Alegria R (2013) Study of a rockfall in a limy conglomerate canyon (Covarrubias, Burgos, N. Spain). Environ Earth Sci 70:2703–2717. doi:10.1007/s12665-013-2327-x

Alemdag S, Akgun A, Kaya A, Gökçeoğlu C (2014) A large and rapid planar failure: causes, mechanism, and consequences (Mordut, Gumushane, Turkey). Arab J Geosci 7:1205–1221

Anon OH (1979) Classification of rocks, and soils for engineering geological mapping. Part I-rock and soil materials. Bull Int Ass Eng Geol 19:364–371

Asteriou P, Saroglou H, Tsiambaos G (2012) Geotechnical and kinematic parameters affecting the coefficients of restitution for rock fall analysis. Int J Rock Mech Min Sci 54:03–113

Binal A, Ercanoğlu M (2010) Assessment of rockfall potential in the Kula (Manisa, Turkey) Geopark Region. Environ Earth Sci 61:1361–1373

Chau KT, Wong RHC, Wu JJ (2002) Coefficient of restitution and rotational motions of rockfall impacts. Int J Rock Mech Min Sci 39:69–77

De Beer JH (1967) Subjective classification of the hardness of rocks and the associated shear strength. In: Proceedings of 4th regional congress afi., soil mechanical found, engineering, Capetown, pp 396–398

Diederichs MS, Hoek E (1989) DIPS 6.01. In: Advanced version computer programme, Rock Engineering Group, Department of Civil Engineering, University of Toronto

Fityus SG, Giacomini A, Buzzi O (2013) The significance of geology for the morphology of potentially unstable rocks. Eng Geol 162:43–52

Fornaro M, Peila D, Nebbia M (1990) Block falls on rock slopes application of a numerical simulation program to some real cases. In: Price DG (ed) Proceedings of the sixth international congress IAEG. Balkema, Amsterdam, pp 2173–2180

Frayssines M, Hantz D (2006) Failure mechanisms and triggering factors in calcareous cliffs of the Subalpine Ranges (French Alps). Eng Geol 86:256–270

Frayssines M, Hantz D (2009) Modelling and back-analysing failures in steep limestone cliffs. Int J Rock Mech Min Sci 46:1115–1123

Göktaş F (1998) Stratigraphy and sedimentology of neogene sedimentation around Muğla (SW Anatolia) (Muğla çevresi (GB Anadolu) Neojen tortullaşmasının stratigrafisi ve sedimantolojisi). Mineral and Research Institute of Turkey (Maden Teknik ve Arama Genel Müdürlüğü) report no 10225, Ankara, Turkey (unpublished, **in Turkish**)

Gül M (2015) Lithological properties and environmental importance of the quaternary colluviums (Mugla, SW Turkey). Environ Earth Sci 74:4089–4108. doi:10.1007/s12665-015-4506-4

Gül M, Karacan E, Aksoy M (2013) An investigation of general geologic and engineering geological properties of Mugla city centre and surrounding (Muğla kenti yerleşim alanı ve yakın çevresinin genel jeolojik ve mühendislik jeolojisi özelliklerinin araştırılması), Mugla Sıtkı Koçman University Research Fund: BAP project no: 12/54. 25p (**in Turkish**)

Hermanns RL, Blikra LH, Naumann M, Nilsen B, Panthi KK, Stromeyer D, Longva O (2006) Examples of multiple rock-slope collapses from Köfels (Ötz valley, Austria) and western Norway. Eng Geol 83:94–108. http://www.muglakulturturizm.gov.tr/TR.73784/mugla.html. Accessed 25 June 2015

Hungr O, Leroueil S, Picarelli L (2014) The Varnes classification of landslide types, an update. Landslides 11:167–194

ISRM (2007) The complete ISRM suggested methods for rock characterization, testing and monitoring: 1974–2006. Suggested methods prepared by the commission on testing methods, ISRM. In: Ulusay R, Hudson JA (eds) Compilations arranged by the ISRM Turkish National Group Ankara, Kozan ofset, Turkey, p 628

Kaya Y, Topal T (2015) Evaluation of rock slope stability for a touristic coastal area near Kusadasi, Aydin (Turkey). Environ Earth Sci 74–5:4187–4199

Keskin İ (2013) Evaluation of rock falls in an urban area: the case of Boğaziçi (Erzincan/Turkey). Environ Earth Sci 70:1619–1628. doi:10.1007/s12665-013-2247-9

Koleini M, Van Rooy JL (2011) Falling rock hazard index: a case study from the Marun Dam and power plant, south-western Iran. Bull Eng Geol Environ 70:279–290

Konak N, Akdeniz N, Öztürk EM (1987) Geology of the south of Menderes massif: IGCP project no. 5: correlation of variscan and pre-variscan events of the Alpine-Mediterranean Mountain Belt. Field meeting, Turkey, 13–19 Sep 1987a, Guide Book For the Field Excursion Along Western Anatolia, Turkey, 42–53, Ankara

Korkanç M, Tuğrul A, Savran A, Özgür FZ (2014) Structural–geological problems in Gümüşler archeological site and monastery. Environ Earth Sci. doi:10.1007/s12665-014-3739-y

Li L, Lan H (2015) Probabilistic modeling of rockfall trajectories: a review. Bull Eng Geol Environ. doi:10.1007/s10064-015-0718-9 **(in press)**

MGM (2015a). http://www.mgm.gov.tr/veridegerlendirme/il-ve-ilceler-istatistik.aspx?m=MUGLA. Accessed 25 June 2015

MGM (2015b). http://www.mgm.gov.tr/veridegerlendirme/yillik-toplam-yagis-verileri.aspx?m=MUGLA. Accessed 25 June 2015

MTA (2002) 1:500.000 scaled geological map of Turkey, Aydın, N20 sheet, Mineral and Research Institute of Turkey (Maden Teknik ve Arama Genel Müdürlüğü) Ankara, Turkey

Ocakoglu F, Acikalin S, Gokceoglu C, Karabacak V, Cherkinsky A (2009) A multistory gigantic subaerial debris flow in an active fault scarp from NW Anatolia: anatomy, mechanism and timing. Holocene 19–6:955–965

Peng B (2000) Rockfall trajectory analysis-parameter determination and application. Thesis of master of science in engineering geology in the University of Canterbury

Richards LR, Peng B, Bell DH (2001) Laboratory and field evaluation of the normal coefficient of restitution for rocks rock mechanics: a challenge for society. In: Särkkä, Eloranta (eds) Proceedings of Eurock Conference, Finland, pp 149–155

Rocscience (2002) RocFall software—for risk analysis of falling rocks on steep slopes. Rocscience User's Guide, p 59

Rocscience (2015). https://rocscience.com/help/dips/webhelp/dips/What_s_New_in_Dips_Version_6.0.htm. Accessed 25 June 2015

Sadagah B (2015) Back analysis of a rockfall event and remedial measures along part of a Mountainous Road, Western Saudi Arabia. Int J Innov Sci Mod Eng (IJISME). ISSN: 2319-6386, 3-2:1-7

Saroglou H, Marinos V, Marinos P, Tsiambaos G (2012) Rockfall hazard and risk assessment: an example from a high promontory at the historical site of Monemvasia, Greece. Nat Hazards Earth Syst Sci 12:1823–1836. doi:10.5194/nhess-12-1823-2012

Sezer İL (2003) Seismic risk and activity in Muğla region (Muğla yöresinde deprem aktivitesi ve riski). IV. Quaternary Colloqium-Kuvaterner Çalıştayı. Istanbul Technical University-Eurasian Earth Science Institute (İTÜ Avrasya Yerbilimleri Enstitüsü), 111–120 (**in Turkish**)

Tang H, Crosta GB, Wang F (2014) Preface special issue on advances in engineering geology for landslides and slope stability problems: part I. Eng Geol 182:1–2

Topal T, Akın M, Özden AU (2006) Analysis and evaluation of rockfall hazard around Afyon Castle, Turkey. In: Proceedings of 10th international congress IAEG 2006- engineering geology for tomorrow's cities, p 7

Topal T, Akin MK, Akin M (2012) Rockfall hazard analysis for an historical Castle in Kastamonu (Turkey). Nat Hazards 62:255–274. doi:10.1007/s11069-011-9995-1

Varnes DJ (1978) Slope movement types and processes. In: Schuster RL, Krizek RJ (eds) Landslides: analysis and control. Special report 176, Transportation and Road Research Board, National Academy of Science, Washington, pp 11–33

Wasowski J, Gaudio VD (2000) Evaluating seismically induced mass movement hazard in Caramanico Terme (Italy). Eng Geol 58:291–311

Wei LW, Chen H, Lee CF, Huang WK, Lin ML, Chi CC, Lin HH (2014) The mechanism of rockfall disaster: a case study from Badouzih, Keelung, in northern Taiwan. Eng Geol 183:116–126

Wu SS (1985) Rockfall evaluation by computer simulation. Transp Res Rec 1031:1–5

Wyllie DC, Mah C (2004) Rock slope engineering, civil and mining engineering, 4th edn. CRC Press, Boca Raton, p 456

Yılmaz I, Yıldırım M, Keskin İ (2008) A method for mapping the spatial distribution of RockFall computer program analyses results using ArcGIS software. Bull Eng Geol Environ 67:547–554

Zorlu K, Tunusluoglu MC, Gorum T, Nefeslioglu HA, Yalcin A, Turer D, Gokceoglu C (2011) Landform effect on rockfall and hazard mapping in Cappadocia (Turkey). Environ Earth Sci 62:1685–1693